6th IEEE RAS/EMBS International Conference on
Biomedical Robotics and Biomechatronics (BioRob)
June 26-29, 2016. UTown, Singapore

Ultrasound-Guided Stabilization of a Robotically-Actuated Delivery Sheath (RADS) for Beating Heart Mitral Valve Motions

Gustaaf J. Vrooijink, Mylène P. Jansen, Manon L. Tolhuisen, Jan G. Grandjean and Sarthak Misra

***Abstract*— Minimally invasive mitral valve (MV) repair surgery significantly reduces trauma compared to an open heart procedure, which enables fast recovery and treatment to high-risk patients. However, limited vision and dexterity of the instrument at the treatment location poses a challenge for minimally invasive surgery. Additionally, MV repair surgery performed without cardiopulmonary bypass often requires the surgeon to deal with beating heart motions. By autonomous stabilization of the instrument, a virtually-still treatment location could be provided. This allows the surgeon to perform surgery as if the heart was stopped. In this study, we present and evaluate a framework that assists the surgeon by stabilizing the instrument for the beating heart MV motions. Our work contributes a robotically-actuated delivery sheath (RADS), which is stabilized in a realistic and functional MV model embedded in a heart motion system. The heart motion system is mounted on a six degrees-of-freedom Stewart platform, which reproduces beating heart MV motions based on pre-operative patient data obtained from three-dimensional magnetic resonance and ultrasound images. Experimental results shows stabilization of the RADS in a beating heart MV model with a mean absolute tracking error of 1.31 mm. The presented framework for stabilization of the RADS in the beating heart could be applicable to a wide variety of existing and potential future cardiovascular interventions.**

I. Introduction

Mitral valve (MV) repair is often associated with improved patient survival compared to prosthetic valve implantation [1]. Repair strategies aim to preserve the MV architecture for natural hemodynamics, reducing risk of embolism and minimizing long-term anticoagulation [2]. However, MV repair often entails complex cardiopulmonary bypass surgery with careful intraoperative decision making. Although, the surgical access via sternotomy used in cardiopulmonary bypass surgery is considered to be an advantage, it goes at the expense of severe patient trauma. Hence, patients with comorbidities are often considered a high risk and denied surgery.

The authors are affiliated with the Surgical Robotics Laboratory, Department of Biomechanical Engineering, MIRA-Institute for Biomedical Technology and Technical Medicine, University of Twente, P.O. Box 217, 7500 AE Enschede, The Netherlands. J.G. Grandjean is also affiliated with the Department of Cardiothoracic Surgery, Thorax Center Twente, Koningsplein 1, 7512 KZ Enschede, The Netherlands. S. Misra is also affiliated with the Surgical Robotics Laboratory, Department of Biomedical Engineering, University of Groningen and University Medical Center Groningen, Hanzeplein 1, 9700 RB Groningen, The Netherlands. The authors would like to thank Menno Lageweg for his contribution in development of the Stewart platform. This research is supported by the Dutch Technology Foundation STW (*i*MIT-Instruments for Minimally Invasive Techniques Interactive Multi-Interventional Tools (Project: MULTI)), which is part of the Netherlands Organisation for Scientific Research (NWO) and partly funded by the Ministry of Economic Affairs, Agriculture and Innovation.

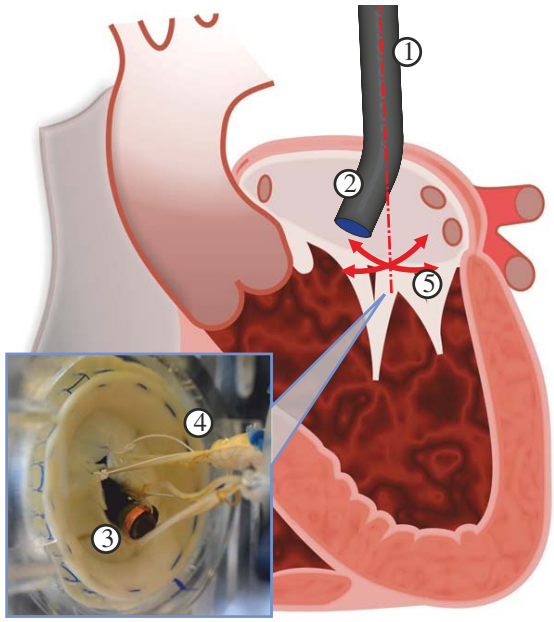

Fig. 1. A robotically-actuated delivery sheath (RADS) ① is inserted into the left atrium of the heart. The RADS tip shown in ② and depicted in the bottom-left inset ③ is introduced into the mitral valve (MV) model ④. MV motion ⑤ is compensated by stabilization of the articulating tip within the annulus. This potentially enables the surgeon to perform complex MV repair procedures while the heart is beating.

As an alternative, minimally invasive MV repair could significantly reduce trauma, which enables fast recovery and treatment to high-risk patients [3]. However, minimally invasive MV repair poses a challenge when it comes to accessibility, vision and dexterity at the treatment location. In addition to the above mentioned challenges, minimally invasive surgery performed without cardiopulmonary bypass often requires the surgeon to deal with beating heart motions. Tracking of the beating heart requires undivided attention of the surgeon, whose accuracy significantly deteriorates for complex repetitive motions up to 60 beats-per-minute (BPM) [4]. By autonomous stabilization of the instrument within the beating heart, a virtually-still treatment location could be obtained, which allows the surgeon to perform surgery as if the heart was stopped.

Several research groups have described (semi)-autonomous insertion, guidance and navigation of steerable catheters [5]–[7]. Although these studies focus on (semi)-autonomous guidance of catheters, their work does not compensate for beating heart motions. Tracking of organ surfaces, including that of a beating heart has been presented by a number of researchers [8]–[11]. However, only a limited number of studies describe autonomous stabilization of the instrument for beating heart motions. *In*

978-1-5090-3287-7/16/$31.00 ©2016 IEEE

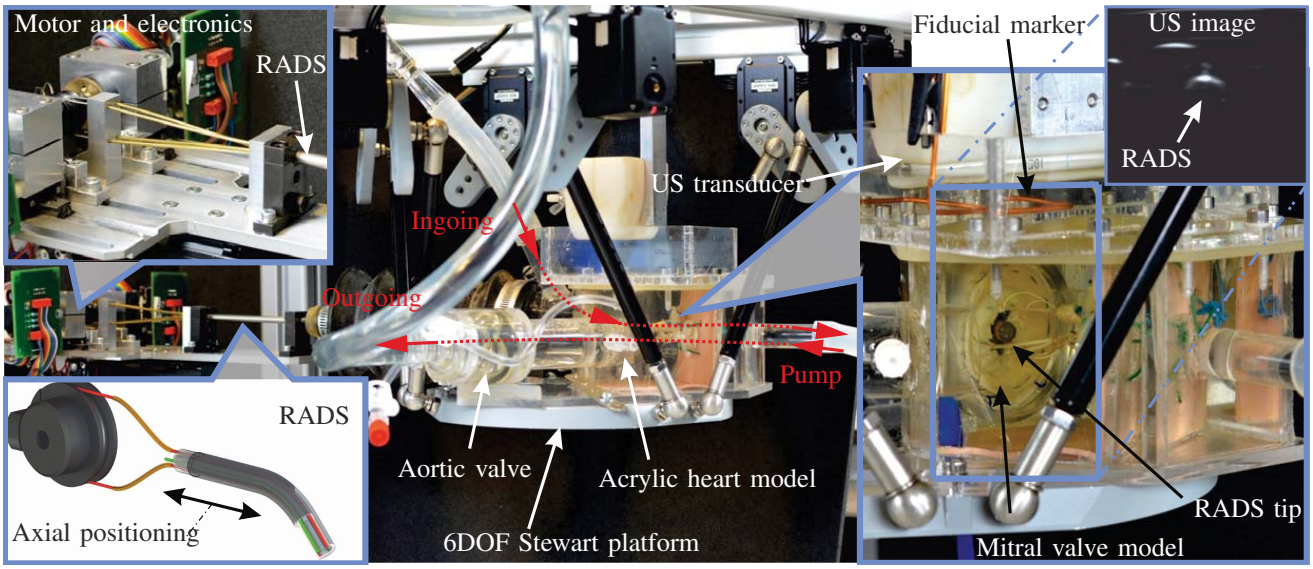

Fig. 2. The experimental setup used to demonstrate stabilization of a robotically-actuated delivery sheath (RADS) for the mitral valve (MV) motions. The RADS (bottom left inset) is inserted into an acrylic heart model (right inset), which is mounted on a six degrees-of-freedom (6DOF) Stewart platform and is used to reproduce beating heart MV motions. The motors and electronics depicted in the top-left inset are attached to the proximal end of the RADS and control the articulating tip in 2DOF. The articulating tip of RADS is inserted into the MV model (shown in the bottom-right inset) in order to compensate for cardiac motion in the annular plane. A two-dimensional (2D) US transducer is positioned along the MV annulus, which shows a radial cross-sectional view of the RADS as depicted in the top-right inset. A manually-operated pump is used to obtain an ingoing fluid flow through the MV into the left ventricle and subsequently an outgoing fluid flow by exiting via the aortic valve (indicated by red arrows).

vivo tracking and compensation of surface motion using a camera has been presented by Gangloff et al. [12]. Kesner et al. demonstrated autonomous stabilization within the beating heart by applying a constant force against a moving target assisted by force and ultrasound (US) feedback [13]. Further, Bowthorpe et al. describe a tele-operated US-guided catheter which is used to anticipate for cardiac motions [14]. Note, that the above mentioned studies address one-dimensional motion compensation (along the instrument insertion axis), while a wide variety of future and existing MV repair procedures could benefit from dexterity and compensation perpendicular to the instrument shaft [15].

In this study, we develop a framework that assists the surgeon by stabilizing the instrument for the beating heart MV motions in two-dimensions (2D) (Fig. 1). Our work contributes an integrated system that demonstrates tracking and control of a robotically-actuated delivery sheath (RADS) in a realistic and functional MV model. An acrylic heart system with an embedded MV model is attached to a six degrees-of-freedom (6DOF) Stewart platform, which reproduces motions based on pre-operative patient data obtained from three-dimensional (3D) magnetic resonance (MR) and US images. Further, a manually-operated heart pump is integrated to provide fluid flow, which enables opening and closure of the MV model.

To the best of our knowledge, we are the first to experimentally demonstrate a novel US-guided system to autonomous stabilize the RADS in a realistic and functional MV model. Our system is capable of accurately tracking and stabilizing the RADS for the MV motions, which potentially assists the surgeon in beating heart surgery. Applications that could benefit from such an autonomous system include MV repair, ablation and cardiovascular biopsies.

II. Methods

In this section, we present the methods used to demonstrate stabilization of the RADS for MV motions. In section II-A, we provide details of the experimental setup. Subsequently, Section II-B describes segmentation and coordinate transformations used in autonomous control of the RADS. In Section II-C, we present the US-guided controller to facilitate stabilization using the RADS. Further, in Section II-D, we elaborate on the pre-operative patient data obtained from 3D MR and US images, which are used in experiments.

A. Experimental Setup

The experimental setup comprises of a RADS controlled by motors and electronics inside an acrylic heart system with an integrated realistic MV model (Fig. 2). A heart pump is used to mimic flow characteristics, while a 6DOF Stewart platform reproduces beating heart motions. Further, we use an US tracking system for feedback of the RADS and MV model for closed-loop control.

The RADS consists of a tendon-driven design including a rigid shaft, a flexible steerable segment and a rigid link to enable articulating tip movement in 2DOF by two pairs of antagonistically-configured tension wires. Each pair of tension wires is actuated by a single pulley attached to motors and electronics configured to minimize friction. In order to reduce hysteresis in the tendon-driven design, we spring-loaded each pulley. For more details on the design and actuation of RADS, we refer the reader to our previous work [16].

The articulating tip of the RADS is inserted into an acrylic heart system containing a left atrium, MV and a left ventricle. The shaft of the RADS is oriented perpendicular to the MV

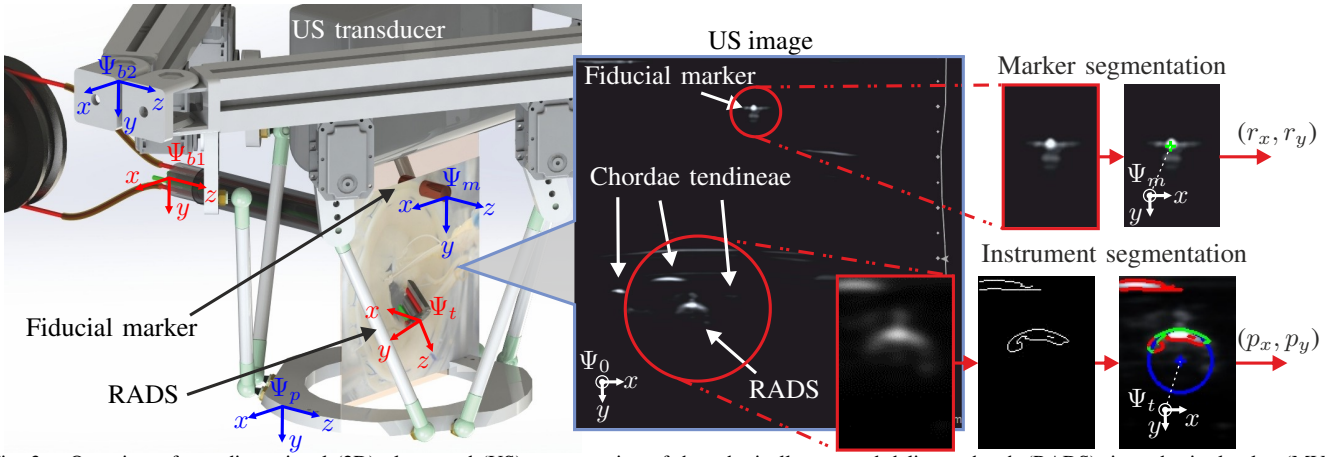

Fig. 3. Overview of two-dimensional (2D) ultrasound (US) segmentation of the robotically-actuated delivery sheath (RADS) tip and mitral valve (MV) positions. The US transducer is positioned along the MV annular plane, which shows a radial cross-sectional view of the RADS tip, chordae tendineae and a MV fiducial marker. The centroid of the fiducial marker attached to the MV model is evaluated as the green cross (top right inset) and considered as a reference signals (i_x and i_y) in closed-loop control. The RADS tip position is evaluated as the center of the blue circle (p_x, p_y) shown in the bottom right inset by using segmentation techniques such as Gaussian filtering, Canny edge detection and a random sample consensus algorithm, where green (inliers) and red (outliers) describe the semi-circular surface. Note, that soft tissue such as the chordae tendineae evaluated as part of the edge map is considered to be an outlier to the RADS semi-circular surface. The coordinate systems attached to various parts of the RADS, heart motion system and US segmentation are depicted red, blue and white, respectively. The frame (Ψ_{b1}) is attached to the base of the RADS, while frame (Ψ_t) is fixed to the tip. The frame (Ψ_{b2}) is assigned to the base of the Stewart platform and frame (Ψ_p) is fixed to its end-effector platform, while frame (Ψ_m) is associated with the MV fiducial marker. The RADS tip (frame (Ψ_t)) and MV fiducial marker (frame (Ψ_t)) are expressed in the US image (frame (Ψ_0)) by segmentation.

annulus. Further, the atrium and ventricle of the acrylic heart system are separated by a realistic MV model (LifeLike BioTissue Inc., London, Canada), which is used in MV repair training. The chordae tendineae of the MV model are attached to the wall of the acrylic heart system to enable valve opening and closure.

A manually-operated ABIOMED AB5000$^{\text{TM}}$ heart pump (ABIOMED, Inc, Danvers, USA) is attached to the left ventricle of the acrylic heart system in order to enable opening and closing of the MV model. We use water as a fluid to mimic flow characteristics of the heart. Ventricular filling is initiated by the pump, where the fluid flows from the left atrium through the open MV into the left ventricle. Subsequently, the MV closes by ventricular ejection of the fluid from the ventricle into the aorta through the aortic valve.

The acrylic heart system is attached to a 6DOF Stewart platform, which is used to reproduce the beating heart MV motions along the MV annular plane. The integrated MV motions are obtained by pre-operative patient data using 3D MR and US imaging. The 6DOF Stewart platform is actuated by six MX-64AR servo motors (ROBOTIS Co., Ltd., Seoul, South Korea) and reproduces the beating heart MV motions as a stand-alone system.

A Siemens Acuson S2000$^{\text{TM}}$ US system (Siemens AG, Erlangen, Germany) is used to provide feedback for the autonomous control. A Siemens 18L6 transducer operating with a frequency of 16 MHz, a scanning depth of 6.5 cm and an image resolution of 0.12 mm per pixel is positioned along the MV annular plane. This provides a radial cross-sectional view of the RADS tip within the MV annular plane. The transducer is partly submerged in a water container on top of the MV and is stationary with respect to the moving acrylic heart system and RADS tip. Note, that a fixed transducer position leads to simplifications with respect to a clinical scenario. The US images are transferred for segmentation via an Epiphan DVI2USB3.0 frame grabber (Epiphan Systems Inc, Ottawa, Canada) to a computer (3.30 GHz Intel® I7-5820K, 16-GB internal memory and 64-bit Windows 7) with a frame rate of 30 frames-per-second. Note, that the transthoracic echocardiography approach used in this study could be replaced by a transesophageal echocardiography (TEE) without any modifications in our segmentation methods.

B. Segmentation

This section describes the segmentation techniques applied to evaluate the RADS tip and the MV positions in the 2D US images (Fig. 3). The visibility of the RADS tip is enhanced by increasing the acoustic impedance difference at the interface between instrument and surrounding materials. The acoustic impedance of a material is given by $Z = \rho c$, where ρ denotes its density and c its acoustic velocity. A reflection coefficient described by acoustic impedance difference at an interface between two materials can be computed according to

$$r = \left(\frac{\rho_2 c_2 - \rho_1 c_1}{\rho_2 c_2 + \rho_1 c_1} \right)^2 . \tag{1}$$

Thus, by considering the material properties of water ($\rho_1 = 988$ kg/m^3 and $c_1 = 1497$ m/s) and copper ($\rho_2 = 8960$ kg/m^3 and $c_2 = 3810$ m/s), we add a thin copper film to the tip of the RADS, which causes a reflection ($r = 84\%$) of the US waves [17]. Note, that the acoustic impedance of water and blood ($\rho_b = 1025$ kg/m^3 and $c_b = 1570$ m/s) are approximately the same. Similarly, we attach a cylindrical copper fiducial marker to the MV model. The enhanced visibility of the MV model improves motion tracking, which could also be considered in clinical practice. Note, that the copper used in this study could be replaced by biocompatible materials such as gold ($\rho = 19290$ kg/m^3 and $c = 3240$ m/s), which is often used as a fiducial marker.

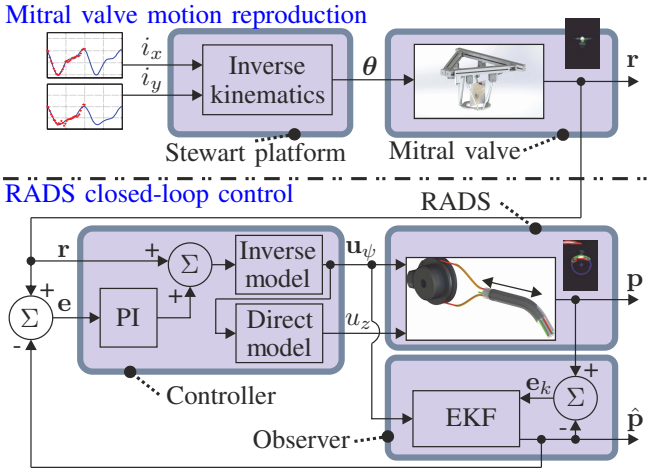

Fig. 4. Overview of the closed-loop control strategy used to stabilize the robotically-actuated delivery sheath (RADS) for the mitral valve (MV) motions. A Stewart platform with joint angles ($\boldsymbol{\theta}$) is used to reproduce the beating heart MV motions (i_x and i_y). The measured MV position ($\mathbf{r}$) is considered as a reference in closed-loop control of the RADS. The signals $\mathbf{u}_\psi = [\psi_x \ \psi_y]^T$ and u_z are used to control the RADS pulleys and axial positioning, respectively. An extended Kalman filter (EKF) is integrated to provide a filtered RADS tip position ($\hat{\mathbf{p}} = [\hat{p}_x \ \hat{p}_y]^T$) of the measurement ($\mathbf{p} = [p_x \ p_y]^T$), which is updated by feedback signal ($\mathbf{e}_k = \mathbf{p} - \hat{\mathbf{p}}$). A proportional and integral control action is used to address the reference tracking error ($\mathbf{e} = \mathbf{r} - \hat{\mathbf{p}}$).

In order to track the RADS tip in 2D US images, we evaluate the semi-circular shape that describes its reflecting surface. We use a 2D Gaussian kernel to reduce speckle and smoothen edges in the US image. Due to variations in contrast of the US image caused by differences in the acoustic impedances between the RADS and the surrounding materials, we apply a Canny edge detector with hysteresis thresholding to obtain an edge map. However, irrelevant edges introduced by surrounding tissue and RADS surface deformations by imaging artefacts may still exist. Hence, we apply a random sample consensus strategy (RANSAC) that uses the parametric description of a semi-circle to evaluate the centroid location of the RADS tip (Fig. 3). The RANSAC strategy provides robustness to irrelevant edges that are not evaluated as part of a semi-circle [16].

In order to evaluate the fiducial marker attached to the MV model, we use a blob extraction method. A blob representing the fiducial marker can be described by a circular region of the image in which the contrast is different compared to surrounding regions. This region can be segmented by thresholding and is evaluated using the size of the cross-sectional area, which should be consistent with the fiducial marker. Further, the robustness of fiducial marker segmentation is increased by evaluating the centroid (r_x, r_y) with corresponding contour for circularity.

The segmented RADS tip and MV positions enable coordinate transformations between frames. The coordinate systems corresponding to the experimental setup are described in Fig. 3. The coordinate transformation between tip frame (Ψ_t) and base frame (Ψ_{b1}) of the RADS can be described by direct and inverse kinematic relations. Similarly, the coordinate transformations between fiducial marker frame (Ψ_m), effector frame (Ψ_p) and base frame (Ψ_{b2}) of the

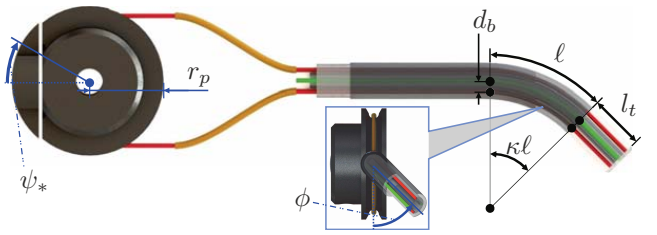

Fig. 5. An overview of the robotically-actuated delivery sheath (RADS) driven by a two pulleys with fixed radii (r_p) and angles (ψ_x and ψ_y), where ℓ is the flexible segment length, l_t denotes the rigid link and d_b is the tendon moment arm with respect to the instrument backbone. The bending direction is given by ϕ, while the bend curvature is presented by κ.

moving MV system are given by kinematics. Note, that the transformation between end effector frame (Ψ_p) and fiducial marker frame (Ψ_m) is considered to be a constant.

Registration of the RADS tip frame (Ψ_t) and MV fiducial marker frame (Ψ_m) in the US image frame (Ψ_0) are provided by US segmentation. Registration allows for the coordinate systems associated with the RADS (red in Fig. 3) and the coordinate systems attached to the moving MV system (blue in Fig. 3) to be expressed in a common coordinate system (frame (Ψ_0)), which is used for US-guided control.

C. Ultrasound-guided control

The US-guided controller used to stabilize the RADS for the MV motions is shown in Fig. 4. The experimental setup consists of two independently controlled systems: A 6DOF Stewart platform controlled to reproduce the MV motions along the MV annular plane (x- and y-axes frame (Ψ_{b2})) and a RADS used to stabilize for the MV motions.

A 6DOF Stewart platform controlled by joint angles ($\boldsymbol{\theta} \in \mathbb{R}^6$, where $\boldsymbol{\theta} = [\theta_1 \ \cdots \ \theta_6]^T$ is used to reproduce the beating heart MV motions in the annular plane by using the inverse kinematics [18]. The joint angles ($\boldsymbol{\theta}$) obtained by inverse kinematics consider the MV reference signals (i_x) and (i_y) provided by pre-operative patient data obtained from 3D MR and US images, which is described in Section II-D. Note, that no MV motion by along the z-axis (frame Ψ_{b2}) is reproduced by the end-effector of the Stewart platform. The motion of the MV model is registered in US images by segmentation of a fiducial marker, which is used as a reference signal ($\mathbf{r} \in \mathbb{R}^2$, where $\mathbf{r} = [r_x \ r_y]^T$) for closed-loop control of the RADS. Note, that the MV motion reproduction is independently controlled and reference signals (i_x) and (i_y) are not provided as an input to the RADS controller.

The RADS is driven by motorized pulleys with fixed radius (r_p) (Fig. 5). By controlling the pulley angles ($\boldsymbol{u}_\psi \in \mathbb{R}^2$, where $\boldsymbol{u}_\psi = [\psi_x \ \psi_y]^T$), we provide articulating tip positioning in the annulus of the MV model. A closed-loop control strategy is used to stabilize the RADS for the MV motions by using the direct and inverse kinematics [16]. The direct kinematics ($\mathbf{H}_t^{b1} \in SO3$) of the RADS is given by

$$\mathbf{H}_t^{b1} = \begin{bmatrix} c_\phi c_{\kappa\ell} & -s_\phi & c_\phi s_{\kappa\ell} & c_\phi \left(\frac{(1-c_{\kappa\ell})}{\kappa} + l_t s_{\kappa\ell} \right) \\ s_\phi c_{\kappa\ell} & c_\phi & s_\phi s_{\kappa\ell} & s_\phi \left(\frac{(1-c_{\kappa\ell})}{\kappa} + l_t s_{\kappa\ell} \right) \\ -s_{\kappa\ell} & 0 & c_{\kappa\ell} & \frac{s_{\kappa\ell}}{\kappa} + l_t c_{\kappa\ell} \\ 0 & 0 & 0 & 1 \end{bmatrix}, \quad (2)$$

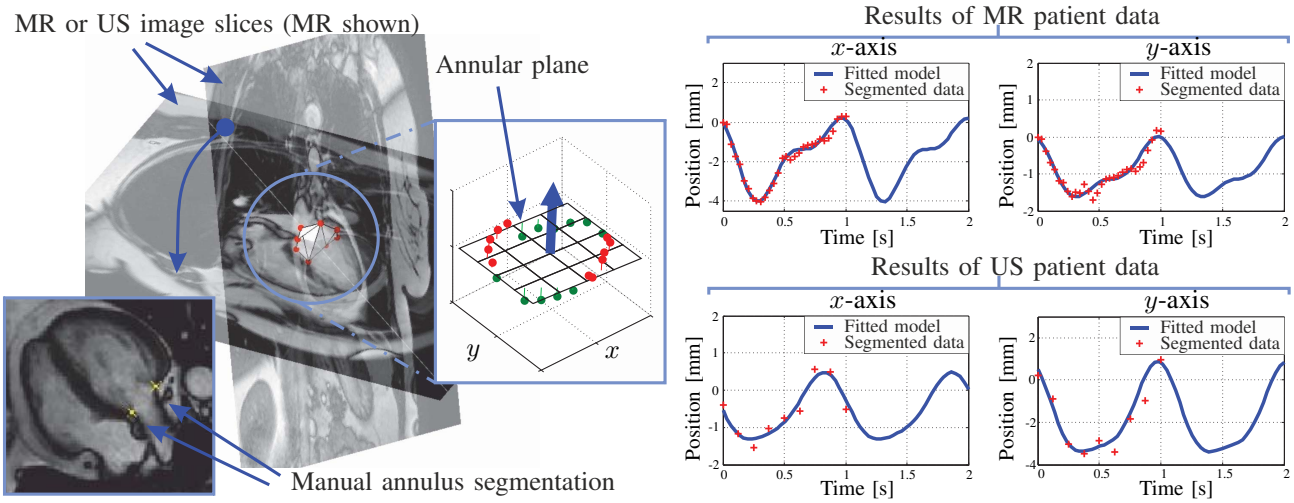

Fig. 6. Overview of mitral valve (MV) motion modeling using pre-operative patient data obtained from three-dimensional (3D) magnetic resonance (MR) and ultrasound (US) images. By manual segmentation of the MV annulus in cross-sectional images as depicted in the bottom-left inset, we evaluate the annular plane as demonstrated in the center inset. Evaluation of the MV annulus positions during the cardiac cycle provides motion data from two independent sources along the x- and y-axes of the annular plane, which is shown in the top and bottom graphs for MR and US patient data, respectively.

where $c_* = \cos(*)$, $s_* = \sin(*)$, ℓ denotes the flexible segment length, l_t is the rigid link length, ϕ describes the RADS bending direction according to

$$\phi = \arctan\left(\frac{\psi_y}{\psi_x}\right), \tag{3}$$

while κ is the curvature of the flexible segment given by

$$\kappa = \frac{r_p\sqrt{\psi_x^2 + \psi_y^2}}{\ell d_b}, \tag{4}$$

where d_b the tendon moment arm with respect to the instrument backbone. Further, given a desired tip position ($\mathbf{d}_t^{b1} \in \mathbb{R}^3$, where $\mathbf{d}_t^{b1} = [d_x\ d_y\ d_z]^T$), an expression for the inverse kinematics is provided by

$$\begin{bmatrix}\mathbf{d}_t^{b1}\\ 1\end{bmatrix} = \mathbf{H}_t^{b1}\begin{bmatrix}\mathbf{o}_t\\ 1\end{bmatrix} = \begin{bmatrix} c_\phi\left(\frac{(1-c_{\kappa\ell})}{\kappa} + l_t s_{\kappa\ell}\right)\\ s_\phi\left(\frac{(1-c_{\kappa\ell})}{\kappa} + l_t s_{\kappa\ell}\right)\\ \frac{s_{\kappa\ell}}{\kappa} + l_t c_{\kappa\ell}\\ 1\end{bmatrix}, \tag{5}$$

where $\mathbf{o}_t = [0\ 0\ 0]^T$ describes the origin ($\mathbf{o}_t \in \mathbb{R}^3$) of the articulating tip frame (Ψ_t). By substituting the RADS bending direction described by

$$\phi = \arctan\left(\frac{d_y}{d_x}\right), \tag{6}$$

into (5), we can numerically solve for the curvature (κ), while the corresponding pulley angles are provided by

$$\begin{bmatrix}\psi_x\\ \psi_y\end{bmatrix} = \kappa\frac{\ell d_b}{r_p}\begin{bmatrix}cos(\phi)\\ sin(\phi)\end{bmatrix}, \tag{7}$$

which completes the inverse kinematics.

By considering the segmented MV reference signal ($\mathbf{r}$) and the inverse kinematics of the RADS, we can compute the pulley angles ($\boldsymbol{u}_\psi$), which are provided as an input to the RADS. By US segmentation, we obtain the RADS tip position ($\mathbf{p} \in \mathbb{R}^2$, where $\mathbf{p} = [p_x\ p_y]^T$). Note, that US images are often prone to noise and the RADS tip may not always be detected due to occlusions and disturbances. Hence, we integrate an extended Kalman filter (EKF), which is updated by feedback signal ($\mathbf{e}_k \in \mathbb{R}^2$, where $\mathbf{e}_k = \mathbf{p} - \hat{\mathbf{p}}$). The EKF is used to reduce noise and to provide RADS tip position estimation ($\hat{\mathbf{p}} \in \mathbb{R}^2$, where $\hat{\mathbf{p}} = [\hat{p}_x\ \hat{p}_y]^T$) in closed-loop control. The MV reference tracking error ($\mathbf{e}$) caused by disturbances such as flow in the acrylic heart system can be evaluated using the RADS tip position ($\hat{\mathbf{p}}$) according to

$$\mathbf{e} = \mathbf{r} - \hat{\mathbf{p}}. \tag{8}$$

The MV reference tracking error ($\mathbf{e} \in \mathbb{R}^2$) is addressed by a proportional and integral control action. In order to prevent the articulating tip of the RADS to deflect out of the 2D US image plane, we use an additional control signal (u_z) for axial positioning of the RADS along the z-axis (frame Ψ_{b1}). The control signal (u_z) is evaluated by using the direct kinematics, which considers the control action ($\boldsymbol{u}_\psi = [\psi_x\ \psi_y]^T$) as an input to compute the out-of-plane motion.

D. Mitral valve motion modeling

An overview of MV motion modeling based on 3D pre-operative patient data is given in Fig. 6. MV motion modeling is used to experimentally evaluate stabilization of the RADS in a realistic and functional MV model. We manually segment the MV annulus for seven and twelve cross-sectional slices obtained at a rate of 30 and 9 volumes-per-second using a 1.5 Tesla MR imaging scanner and a TEE system (Philips Healthcare, Amsterdam, The Netherlands), respectively. The segmented points of the MV annulus are evaluated by using principle component analysis [19], [20]. The MV annular plane is the span of two eigenvectors of the covariance matrix with the largest variance (i.e., first and second principal components). Further, the normal vector of the annular plane is described by the eigenvector with the least amount of variance, which completes the coordinate system of the MV.

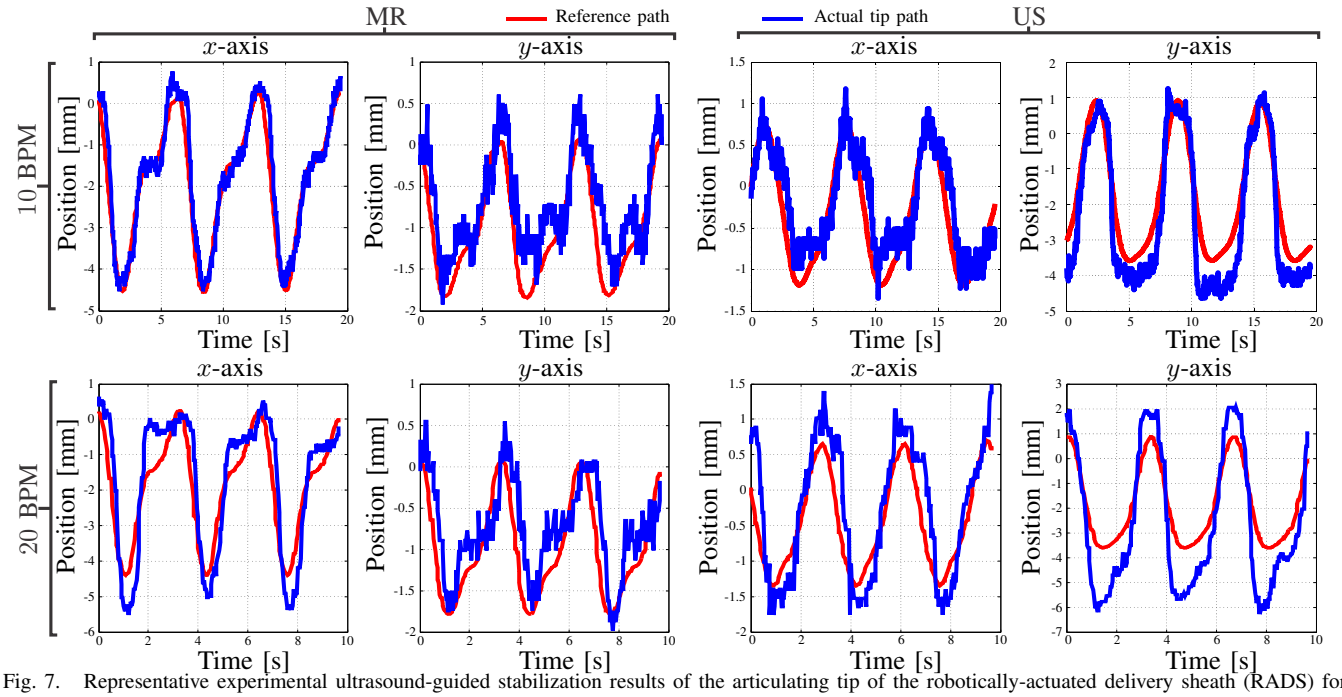

Fig. 7. Representative experimental ultrasound-guided stabilization results of the articulating tip of the robotically-actuated delivery sheath (RADS) for beating heart mitral valve (MV) motions based on MR and US pre-operative patient data for heart rates of 10 and 20 BPM. The red line describes the reference path ($\mathbf{r} = [r_x \; r_y]^T$) obtained from fiducial marker segmentation described in Section II-B, while the blue line represents the actual path ($\mathbf{p} = [p_x \; p_y]^T$) of the RADS tip during experiments. ***Please refer to the accompanying video that demonstrates the results of RADS tip stabilization.***

A model capable of describing the periodic motion of the MV annulus during the cardiac cycle is given by a two-term Fourier series according to

$$i_x = a_{0_x} + a_{1_x} c_{\frac{k}{S_r}\omega} + b_{1_x} s_{\frac{k}{S_r}\omega} + a_{2_x} c_{2\frac{k}{S_r}\omega} + b_{2_x} s_{2\frac{k}{S_r}\omega}, \quad (9)$$

and

$$i_y = a_{0_y} + a_{1_y} c_{\frac{k}{S_r}\omega} + b_{1_y} s_{\frac{k}{S_r}\omega} + a_{2_y} c_{2\frac{k}{S_r}\omega} + b_{2_y} s_{2\frac{k}{S_r}\omega}, \quad (10)$$

where k is the discrete time, S_r describes the sample rate and ω denotes the frequency of the periodic motion. Further, the coefficients obtained from data fitting are provided in Table I, which completes the models evaluated from MR and US data. The periodic signals (i_x and i_y) depicted in Fig. 6 are provided as an input to the Stewart platform, which are used in experiments to reproduce MV motions along the annular plane.

III. Experiments

In this section, the experimental plan is described and the accuracy results of RADS stabilization for the beating heart MV motions are presented.

TABLE I

Table of Fourier coefficients used in (9) and (10) to describe the periodic mitral valve motions obtained from magnetic resonance (MR) and ultrasound (US) images. Subscript * denotes the x- or y-axis, while the corresponding goodness of fit is given by the square of the correlation (R^2).

	axis	a_{0_*}	a_{1_*}	b_{1_*}	a_{2_*}	b_{2_*}	ω	R^2
US	x	-0.550	0.120	-0.871	-0.116	-0.115	2π	0.87
	y	-1.700	1.813	-0.985	0.410	-0.321	2π	0.96
MR	x	-1.735	0.888	-1.413	0.804	-0.006	2π	0.98
	y	-0.906	0.584	-0.363	0.273	-0.050	2π	0.93

A. Experimental plan

Experiments are conducted to evaluate the performance of the presented US-guided system. The articulating tip of the RADS is inserted in a realistic and functional MV model to stabilize the reproduced beating heart MV motions along the MV annular plane (x and y-axes frame (Ψ_{b2})). The motion paths (i_x and i_y) depicted in Fig. 6 are provided as an input to the Stewart platform. We reproduce the beating heart MV motions during experiments for heart rates of 5, 10, 15 and 20 BPM. During experiments we use a manually-operated heart pump to integrate flow characteristics acting on the RADS and MV opening and closing.

B. Results

The results of the experiments conducted are provided in Table II. Further, a representative of MR and US reproduced MV motions experiments for 10 and 20 BPM are shown in Fig. 7. The experiments were repeated five times to evaluate the RADS tip tracking accuracy in the moving MV model. Experiments show a mean absolute positioning errors of 0.68 mm and 1.25 mm along the x- and y-axes (Fig. 7), respectively. Further, we observe a mean absolute tracking error of 1.31 mm for experiments using US pre-operative patient data with a reproduced heart rate of 20 BPM.

Experiments show a deterioration in tracking accuracy for faster heart rates compared to slower heart rates, which could be explained by bandwidth limitations of the closed-loop control system to cope with the reference signal. Further, we observe a significant overshoot in the x-axis in case of MR and the y-axis in case of US motion-path experiments conducted at heart rates of 20 BPM. This could be the delayed observations of the MV fiducial marker, which is

TABLE II

EXPERIMENTAL RESULTS OF THE ROBOTICALLY-ACTUATED DELIVERY SHEATH (RADS) TIP STABILIZATION FOR THE BEATING HEART MITRAL VALVE MOTIONS. THE MEAN ABSOLUTE DISTANCE ERROR (ϵ) AND POSITION ERRORS (ϵ_x AND ϵ_y) ALONG THE x- AND y-AXES ARE PROVIDED. FURTHER, THE STANDARD DEVIATION FOR FIVE REPETITIONS IS REPORTED. ***Please refer to the accompanying video that demonstrates the results of RADS tip stabilization.***

	BPM	ϵ_x [mm]	ϵ_y [mm]	ϵ [mm]
MR	5	0.30 ± 0.02	0.29 ± 0.03	0.42 ± 0.02
	10	0.30 ± 0.02	0.32 ± 0.04	0.44 ± 0.02
	15	0.67 ± 0.05	0.26 ± 0.03	0.72 ± 0.04
	20	0.68 ± 0.10	0.37 ± 0.03	0.78 ± 0.09
US	5	0.33 ± 0.02	0.63 ± 0.03	0.71 ± 0.03
	10	0.25 ± 0.02	0.69 ± 0.06	0.73 ± 0.07
	15	0.41 ± 0.03	0.91 ± 0.17	1.00 ± 0.16
	20	0.41 ± 0.04	1.25 ± 0.08	1.31 ± 0.06

considered to be significant for faster heart rates. Hence, we limit experimental stabilization of the RADS for MV motions to heart rates up of 20 BPM. However, it can not be ruled out that some of these effects could be due to the fluid flow and opening and closing of the MV model, which acts as a disturbance. Further, cross-talk between the two tendon pairs and mechanical friction in the steering mechanism of the RADS could also contribute to the tracking error.

IV. CONCLUSIONS AND FUTURE WORK

In this study, we present a novel approach to stabilize the RADS for beating heart MV motions. We develop segmentation and US-guided control methods, which are used to stabilize the RADS tip within the MV annulus. In order to accurately evaluate the performance of the proposed system, we use a setup that comprises of a realistic and functional MV model. Further, 3D pre-operative MR and US patient data are evaluated and used to reproduce beating heart MV motions. This provides a realistic scenario, which we use to evaluate our integrated system. We experimentally evaluate the novel US-guided system to stabilize the RADS for MV motions. The experiments show a mean absolute tracking error of 1.31 mm for beating heart MV motions evaluated at a heart rate of 20 BPM.

In future work, we aim to expand our 2D US segmentation methods to 3D, which enables tracking of instrument and tissue by using a hand-held transducer. Further, we intend to integrate control strategies capable of anticipation and prediction of beating heart valve motions. This could reduce the tracking error and enable stabilization for MV motions up to 60 BPM. Nonetheless, our presented framework describes a closed-loop controlled US-guided system that demonstrates stabilization of the RADS for beating heart valve motions up to 20 BPM. The proposed system with appropriate modifications, could potentially improve existing procedures and enable future applications in MV repair surgery.

REFERENCES

[1] R. R. Moss, K. H. Humphries, M. Gao, C. R. Thompson, J. G. Abel, G. Fradet, and B. I. Munt, "Outcome of mitral valve repair or replacement: A comparison by propensity score analysis," *Circulation*, vol. 108, no. 10 suppl 1, pp. II–90–II–97, 2003.

[2] S. F. Bolling, S. Li, S. M. O'Brien, J. M. Brennan, R. L. Prager, and J. S. Gammie, "Predictors of mitral valve repair: Clinical and surgeon factors," *The Annals of Thoracic Surgery*, vol. 90, no. 6, pp. 1904–1912, 2010.

[3] J. Y. Woo, E. Rodriguez, P. Atluri, and W. R. Chitwood, Jr, "Minimally invasive, robotic, and off-pump mitral valve surgery," *Seminars in Thoracic and Cardiovascular Surgery*, vol. 18, no. 2, pp. 139–147, 2006.

[4] V. Falk, "Manual control and tracking a human factor analysis relevant for beating heart surgery," *The Annals of Thoracic Surgery*, vol. 74, no. 2, pp. 624–628, 2002.

[5] J. Jayender, R. V. Patel, and S. Nikumb, "Robot-assisted active catheter insertion: Algorithms and experiments," *The International Journal of Robotics Research*, vol. 28, no. 9, pp. 1101–1117, 2009.

[6] Y. Ganji, F. Janabi-Sharifi, and A. N. Cheema, "Robot-assisted catheter manipulation for intracardiac navigation," *International Journal of Computer Assisted Radiology and Surgery*, vol. 4, no. 4, pp. 307–315, 2009.

[7] P. Loschak, L. Brattain, and R. Howe, "Automated pointing of cardiac imaging catheters," in *Proceedings of the IEEE International Conference on Robotics and Automation (ICRA)*, pp. 5794–5799, Karlsruhe, Germany, May 2013.

[8] T. Ortmaier, M. Groger, D. Boehm, V. Falk, and G. Hirzinger, "Motion estimation in beating heart surgery," *IEEE Transactions on Biomedical Engineering*, vol. 52, no. 10, pp. 1729–1740, 2005.

[9] R. Richa, A. Bó, and P. Poignet, "Beating heart motion prediction for robust visual tracking," in *Proceedings of the IEEE International Conference on Robotics and Automation (ICRA)*, pp. 4579–4584, Anchorage, USA, May 2010.

[10] E. Tuna, T. Franke, O. Bebek, A. Shiose, K. Fukamachi, and M. Cavusoglu, "Heart motion prediction based on adaptive estimation algorithms for robotic-assisted beating heart surgery," *IEEE Transactions on Robotics*, vol. 29, no. 1, pp. 261–276, 2013.

[11] P. Moreira, N. Zemiti, C. Liu, and P. Poignet, "Viscoelastic model based force control for soft tissue interaction and its application in physiological motion compensation," *Computer Methods and Programs in Biomedicine*, vol. 116, no. 2, pp. 52–67, 2014.

[12] J. Gangloff, R. Ginhoux, M. de Mathelin, L. Soler, and J. Marescaux, "Model predictive control for compensation of cyclic organ motions in teleoperated laparoscopic surgery," *IEEE Transactions on Control Systems Technology*, vol. 14, no. 2, pp. 235–246, 2006.

[13] S. B. Kesner and R. D. Howe, "Robotic catheter cardiac ablation combining ultrasound guidance and force control," *The International Journal of Robotics Research*, vol. 33, no. 4, pp. 631–644, 2014.

[14] M. Bowthorpe, A. Alvarez Garcia, and M. Tavakoli, "GPC-based teleoperation for delay compensation and disturbance rejection in image-guided beating-heart surgery," in *Proceedings of the IEEE International Conference on Robotics and Automation (ICRA)*, pp. 4875–4880, Hong Kong, China, May 2014.

[15] F. Maisano, O. Alfieri, S. Banai, M. Buchbinder, A. Colombo, V. Falk, T. Feldman, O. Franzen, H. Herrmann, S. Kar, K.-H. Kuck, G. Lutter, M. Mack, G. Nickenig, N. Piazza, M. Reisman, C. E. Ruiz, J. Schofer, L. Søndergaard, G. W. Stone, M. Taramasso, M. Thomas, A. Vahanian, J. Webb, S. Windecker, and M. B. Leon, "The future of transcatheter mitral valve interventions: competitive or complementary role of repair vs. replacement?," *European Heart Journal*, vol. 36, no. 26, pp. 1651–1659, 2015.

[16] G. J. Vrooijink, T. T. M. Ellenbroek, P. Breedveld, J. G. Grandjean, and S. Misra, "A preliminary study on using a robotically-actuated delivery sheath (rads) for transapical aortic valve implantation," in *Proceedings of the IEEE International Conference on Robotics and Automation (ICRA)*, pp. 4380–4386, Hong Kong, China, June 2014.

[17] J. Zhu, *Optimization of Matching Layer Design for Medical Ultrasonic Transducer*. PhD thesis, Pennsylvania State University, 2008.

[18] E. Fichter, "A stewart platform-based manipulator: General theory and practical construction," *The International Journal of Robotics Research*, vol. 5, no. 2, pp. 157–182, 1986.

[19] M. L. Tolhuisen, "Three-dimensional spatial movement of the mitral valve." Master's degree in Technical Medicine (Internship Report), Faculty of Science and Technology, University of Twente, The Netherlands, February 2015.

[20] M. P. Jansen, "Three-dimensional translation and rotation of the mitral valve during the cardiac cycle." Master's degree in Technical Medicine (Internship Report), Faculty of Science and Technology, University of Twente, The Netherlands, November 2015.